Fermilab-Pub-08/090-E

Measurement of the forward-backward charge asymmetry and extraction of $\sin^2\theta_W^{\text{eff}}$ in $p\bar{p} \to Z/\gamma^* + X \to e^+e^- + X$ events produced at $\sqrt{s} = 1.96$ TeV

V.M. Abazov[36], B. Abbott[75], M. Abolins[65], B.S. Acharya[29], M. Adams[51], T. Adams[49], E. Aguilo[6], S.H. Ahn[31], M. Ahsan[59], G.D. Alexeev[36], G. Alkhazov[40], A. Alton[64,a], G. Alverson[63], G.A. Alves[2], M. Anastasoaie[35], L.S. Ancu[35], T. Andeen[53], S. Anderson[45], B. Andrieu[17], M.S. Anzelc[53], M. Aoki[50], Y. Arnoud[14], M. Arov[60], M. Arthaud[18], A. Askew[49], B. Åsman[41], A.C.S. Assis Jesus[3], O. Atramentov[49], C. Avila[8], F. Badaud[13], A. Baden[61], L. Bagby[50], B. Baldin[50], D.V. Bandurin[59], P. Banerjee[29], S. Banerjee[29], E. Barberis[63], A.-F. Barfuss[15], P. Bargassa[80], P. Baringer[58], J. Barreto[2], J.F. Bartlett[50], U. Bassler[18], D. Bauer[43], S. Beale[6], A. Bean[58], M. Begalli[3], M. Begel[73], C. Belanger-Champagne[41], L. Bellantoni[50], A. Bellavance[50], J.A. Benitez[65], S.B. Beri[27], G. Bernardi[17], R. Bernhard[23], I. Bertram[42], M. Besançon[18], R. Beuselinck[43], V.A. Bezzubov[39], P.C. Bhat[50], V. Bhatnagar[27], C. Biscarat[20], G. Blazey[52], F. Blekman[43], S. Blessing[49], D. Bloch[19], K. Bloom[67], A. Boehnlein[50], D. Boline[62], T.A. Bolton[59], E.E. Boos[38], G. Borissov[42], T. Bose[77], A. Brandt[78], R. Brock[65], G. Brooijmans[70], A. Bross[50], D. Brown[81], N.J. Buchanan[49], D. Buchholz[53], M. Buehler[81], V. Buescher[22], V. Bunichev[38], S. Burdin[42,b], S. Burke[45], T.H. Burnett[82], C.P. Buszello[43], J.M. Butler[62], P. Calfayan[25], S. Calvet[16], J. Cammin[71], W. Carvalho[3], B.C.K. Casey[50], H. Castilla-Valdez[33], S. Chakrabarti[18], D. Chakraborty[52], K. Chan[6], K.M. Chan[55], A. Chandra[48], F. Charles[19,‡], E. Cheu[45], F. Chevallier[14], D.K. Cho[62], S. Choi[32], B. Choudhary[28], L. Christofek[77], T. Christoudias[43], S. Cihangir[50], D. Claes[67], J. Clutter[58], M. Cooke[80], W.E. Cooper[50], M. Corcoran[80], F. Couderc[18], M.-C. Cousinou[15], S. Crépé-Renaudin[14], D. Cutts[77], M. Ćwiok[30], H. da Motta[2], A. Das[45], G. Davies[43], K. De[78], S.J. de Jong[35], E. De La Cruz-Burelo[64], C. De Oliveira Martins[3], J.D. Degenhardt[64], F. Déliot[18], M. Demarteau[50], R. Demina[71], D. Denisov[50], S.P. Denisov[39], S. Desai[50], H.T. Diehl[50], M. Diesburg[50], A. Dominguez[67], H. Dong[72], L.V. Dudko[38], L. Duflot[16], S.R. Dugad[29], D. Duggan[49], A. Duperrin[15], J. Dyer[65], A. Dyshkant[52], M. Eads[67], D. Edmunds[65], J. Ellison[48], V.D. Elvira[50], Y. Enari[77], S. Eno[61], P. Ermolov[38], H. Evans[54], A. Evdokimov[73], V.N. Evdokimov[39], A.V. Ferapontov[59], T. Ferbel[71], F. Fiedler[24], F. Filthaut[35], W. Fisher[50], H.E. Fisk[50], M. Fortner[52], H. Fox[42], S. Fu[50], S. Fuess[50], T. Gadfort[70], C.F. Galea[35], E. Gallas[50], C. Garcia[71], A. Garcia-Bellido[82], V. Gavrilov[37], P. Gay[13], W. Geist[19], D. Gelé[19], C.E. Gerber[51], Y. Gershtein[49], D. Gillberg[6], G. Ginther[71], N. Gollub[41], B. Gómez[8], A. Goussiou[82], P.D. Grannis[72], H. Greenlee[50], Z.D. Greenwood[60], E.M. Gregores[4], G. Grenier[20], Ph. Gris[13], J.-F. Grivaz[16], A. Grohsjean[25], S. Grünendahl[50], M.W. Grünewald[30], F. Guo[72], J. Guo[72], G. Gutierrez[50], P. Gutierrez[75], A. Haas[70], N.J. Hadley[61], P. Haefner[25], S. Hagopian[49], J. Haley[68], I. Hall[65], R.E. Hall[47], L. Han[7], K. Harder[44], A. Harel[71], J.M. Hauptman[57], R. Hauser[65], J. Hays[43], T. Hebbeker[21], D. Hedin[52], J.G. Hegeman[34], A.P. Heinson[48], U. Heintz[62], C. Hensel[22,d], K. Herner[72], G. Hesketh[63], M.D. Hildreth[55], R. Hirosky[81], J.D. Hobbs[72], B. Hoeneisen[12], H. Hoeth[26], M. Hohlfeld[22], S.J. Hong[31], S. Hossain[75], P. Houben[34], Y. Hu[72], Z. Hubacek[10], V. Hynek[9], I. Iashvili[69], R. Illingworth[50], A.S. Ito[50], S. Jabeen[62], M. Jaffré[16], S. Jain[75], K. Jakobs[23], C. Jarvis[61], R. Jesik[43], K. Johns[45], C. Johnson[70], M. Johnson[50], A. Jonckheere[50], P. Jonsson[43], A. Juste[50], E. Kajfasz[15], J.M. Kalk[60], D. Karmanov[38], P.A. Kasper[50], I. Katsanos[70], D. Kau[49], V. Kaushik[78], R. Kehoe[79], S. Kermiche[15], N. Khalatyan[50], A. Khanov[76], A. Kharchilava[69], Y.M. Kharzheev[36], D. Khatidze[70], T.J. Kim[31], M.H. Kirby[53], M. Kirsch[21], B. Klima[50], J.M. Kohli[27], J.-P. Konrath[23], A.V. Kozelov[39], J. Kraus[65], D. Krop[54], T. Kuhl[24], A. Kumar[69], A. Kupco[11], T. Kurča[20], V.A. Kuzmin[38], J. Kvita[9], F. Lacroix[13], D. Lam[55], S. Lammers[70], G. Landsberg[77], P. Lebrun[20], W.M. Lee[50], A. Leflat[38], J. Lellouch[17], J. Leveque[45], J. Li[78], L. Li[48], Q.Z. Li[50], S.M. Lietti[5], J.G.R. Lima[52], D. Lincoln[50], J. Linnemann[65], V.V. Lipaev[39], R. Lipton[50], Y. Liu[7], Z. Liu[6], A. Lobodenko[40], M. Lokajicek[11], P. Love[42], H.J. Lubatti[82], R. Luna[3], A.L. Lyon[50], A.K.A. Maciel[2], D. Mackin[80], R.J. Madaras[46], P. Mättig[26], C. Magass[21], A. Magerkurth[64], P.K. Mal[82], H.B. Malbouisson[3], S. Malik[67], V.L. Malyshev[36], H.S. Mao[50], Y. Maravin[59], B. Martin[14], R. McCarthy[72], A. Melnitchouk[66], L. Mendoza[8], P.G. Mercadante[5], M. Merkin[38], K.W. Merritt[50], A. Meyer[21], J. Meyer[22,d], T. Millet[20], J. Mitrevski[70], R.K. Mommsen[44], N.K. Mondal[29], R.W. Moore[6], T. Moulik[58], G.S. Muanza[20], M. Mulhearn[70], O. Mundal[22], L. Mundim[3], E. Nagy[15], M. Naimuddin[50], M. Narain[77], N.A. Naumann[35], H.A. Neal[64], J.P. Negret[8], P. Neustroev[40], H. Nilsen[23], H. Nogima[3], S.F. Novaes[5], T. Nunnemann[25], V. O'Dell[50], D.C. O'Neil[6], G. Obrant[40], C. Ochando[16], D. Onoprienko[59], N. Oshima[50], N. Osman[43], J. Osta[55], R. Otec[10], G.J. Otero y Garzón[50], M. Owen[44], P. Padley[80], M. Pangilinan[77], N. Parashar[56], S.-J. Park[22,d], S.K. Park[31], J. Parsons[70], R. Partridge[77], N. Parua[54], A. Patwa[73],

G. Pawloski[80], B. Penning[23], M. Perfilov[38], K. Peters[44], Y. Peters[26], P. Pétroff[16], M. Petteni[43], R. Piegaia[1], J. Piper[65], M.-A. Pleier[22], P.L.M. Podesta-Lerma[33,c], V.M. Podstavkov[50], Y. Pogorelov[55], M.-E. Pol[2], P. Polozov[37], B.G. Pope[65], A.V. Popov[39], C. Potter[6], W.L. Prado da Silva[3], H.B. Prosper[49], S. Protopopescu[73], J. Qian[64], A. Quadt[22,d], B. Quinn[66], A. Rakitine[42], M.S. Rangel[2], K. Ranjan[28], P.N. Ratoff[42], P. Renkel[79], S. Reucroft[63], P. Rich[44], J. Rieger[54], M. Rijssenbeek[72], I. Ripp-Baudot[19], F. Rizatdinova[76], S. Robinson[43], R.F. Rodrigues[3], M. Rominsky[75], C. Royon[18], P. Rubinov[50], R. Ruchti[55], G. Safronov[37], G. Sajot[14], A. Sánchez-Hernández[33], M.P. Sanders[17], B. Sanghi[50], A. Santoro[3], G. Savage[50], L. Sawyer[60], T. Scanlon[43], D. Schaile[25], R.D. Schamberger[72], Y. Scheglov[40], H. Schellman[53], T. Schliephake[26], C. Schwanenberger[44], A. Schwartzman[68], R. Schwienhorst[65], J. Sekaric[49], H. Severini[75], E. Shabalina[51], M. Shamim[59], V. Shary[18], A.A. Shchukin[39], R.K. Shivpuri[28], V. Siccardi[19], V. Simak[10], V. Sirotenko[50], P. Skubic[75], P. Slattery[71], D. Smirnov[55], G.R. Snow[67], J. Snow[74], S. Snyder[73], S. Söldner-Rembold[44], L. Sonnenschein[17], A. Sopczak[42], M. Sosebee[78], K. Soustruznik[9], B. Spurlock[78], J. Stark[14], J. Steele[60], V. Stolin[37], D.A. Stoyanova[39], J. Strandberg[64], S. Strandberg[41], M.A. Strang[69], E. Strauss[72], M. Strauss[75], R. Ströhmer[25], D. Strom[53], L. Stutte[50], S. Sumowidagdo[49], P. Svoisky[55], A. Sznajder[3], P. Tamburello[45], A. Tanasijczuk[1], W. Taylor[6], J. Temple[45], B. Tiller[25], F. Tissandier[13], M. Titov[18], V.V. Tokmenin[36], T. Toole[61], I. Torchiani[23], T. Trefzger[24], D. Tsybychev[72], B. Tuchming[18], C. Tully[68], P.M. Tuts[70], R. Unalan[65], L. Uvarov[40], S. Uvarov[40], S. Uzunyan[52], B. Vachon[6], P.J. van den Berg[34], R. Van Kooten[54], W.M. van Leeuwen[34], N. Varelas[51], E.W. Varnes[45], I.A. Vasilyev[39], M. Vaupel[26], P. Verdier[20], L.S. Vertogradov[36], M. Verzocchi[50], F. Villeneuve-Seguier[43], P. Vint[43], P. Vokac[10], E. Von Toerne[59], M. Voutilainen[68,e], R. Wagner[68], H.D. Wahl[49], L. Wang[61], M.H.L.S. Wang[50], J. Warchol[55], G. Watts[82], M. Wayne[55], G. Weber[24], M. Weber[50], L. Welty-Rieger[54], A. Wenger[23,f], N. Wermes[22], M. Wetstein[61], A. White[78], D. Wicke[26], G.W. Wilson[58], S.J. Wimpenny[48], M. Wobisch[60], D.R. Wood[63], T.R. Wyatt[44], Y. Xie[77], S. Yacoob[53], R. Yamada[50], M. Yan[61], T. Yasuda[50], Y.A. Yatsunenko[36], H. Yin[7], K. Yip[73], H.D. Yoo[77], S.W. Youn[53], J. Yu[78], C. Zeitnitz[26], T. Zhao[82], B. Zhou[64], J. Zhu[72], M. Zielinski[71], D. Zieminska[54], A. Zieminski[54,‡], L. Zivkovic[70], V. Zutshi[52], and E.G. Zverev[38]

(The DØ Collaboration)

[1] *Universidad de Buenos Aires, Buenos Aires, Argentina*
[2] *LAFEX, Centro Brasileiro de Pesquisas Físicas, Rio de Janeiro, Brazil*
[3] *Universidade do Estado do Rio de Janeiro, Rio de Janeiro, Brazil*
[4] *Universidade Federal do ABC, Santo André, Brazil*
[5] *Instituto de Física Teórica, Universidade Estadual Paulista, São Paulo, Brazil*
[6] *University of Alberta, Edmonton, Alberta, Canada, Simon Fraser University, Burnaby, British Columbia, Canada, York University, Toronto, Ontario, Canada, and McGill University, Montreal, Quebec, Canada*
[7] *University of Science and Technology of China, Hefei, People's Republic of China*
[8] *Universidad de los Andes, Bogotá, Colombia*
[9] *Center for Particle Physics, Charles University, Prague, Czech Republic*
[10] *Czech Technical University, Prague, Czech Republic*
[11] *Center for Particle Physics, Institute of Physics, Academy of Sciences of the Czech Republic, Prague, Czech Republic*
[12] *Universidad San Francisco de Quito, Quito, Ecuador*
[13] *LPC, Univ Blaise Pascal, CNRS/IN2P3, Clermont, France*
[14] *LPSC, Université Joseph Fourier Grenoble 1, CNRS/IN2P3, Institut National Polytechnique de Grenoble, France*
[15] *CPPM, Aix-Marseille Université, CNRS/IN2P3, Marseille, France*
[16] *LAL, Univ Paris-Sud, IN2P3/CNRS, Orsay, France*
[17] *LPNHE, IN2P3/CNRS, Universités Paris VI and VII, Paris, France*
[18] *DAPNIA/Service de Physique des Particules, CEA, Saclay, France*
[19] *IPHC, Université Louis Pasteur et Université de Haute Alsace, CNRS/IN2P3, Strasbourg, France*
[20] *IPNL, Université Lyon 1, CNRS/IN2P3, Villeurbanne, France and Université de Lyon, Lyon, France*
[21] *III. Physikalisches Institut A, RWTH Aachen, Aachen, Germany*
[22] *Physikalisches Institut, Universität Bonn, Bonn, Germany*
[23] *Physikalisches Institut, Universität Freiburg, Freiburg, Germany*
[24] *Institut für Physik, Universität Mainz, Mainz, Germany*
[25] *Ludwig-Maximilians-Universität München, München, Germany*
[26] *Fachbereich Physik, University of Wuppertal, Wuppertal, Germany*
[27] *Panjab University, Chandigarh, India*
[28] *Delhi University, Delhi, India*

[29]Tata Institute of Fundamental Research, Mumbai, India
[30]University College Dublin, Dublin, Ireland
[31]Korea Detector Laboratory, Korea University, Seoul, Korea
[32]SungKyunKwan University, Suwon, Korea
[33]CINVESTAV, Mexico City, Mexico
[34]FOM-Institute NIKHEF and University of Amsterdam/NIKHEF, Amsterdam, The Netherlands
[35]Radboud University Nijmegen/NIKHEF, Nijmegen, The Netherlands
[36]Joint Institute for Nuclear Research, Dubna, Russia
[37]Institute for Theoretical and Experimental Physics, Moscow, Russia
[38]Moscow State University, Moscow, Russia
[39]Institute for High Energy Physics, Protvino, Russia
[40]Petersburg Nuclear Physics Institute, St. Petersburg, Russia
[41]Lund University, Lund, Sweden, Royal Institute of Technology and Stockholm University, Stockholm, Sweden, and Uppsala University, Uppsala, Sweden
[42]Lancaster University, Lancaster, United Kingdom
[43]Imperial College, London, United Kingdom
[44]University of Manchester, Manchester, United Kingdom
[45]University of Arizona, Tucson, Arizona 85721, USA
[46]Lawrence Berkeley National Laboratory and University of California, Berkeley, California 94720, USA
[47]California State University, Fresno, California 93740, USA
[48]University of California, Riverside, California 92521, USA
[49]Florida State University, Tallahassee, Florida 32306, USA
[50]Fermi National Accelerator Laboratory, Batavia, Illinois 60510, USA
[51]University of Illinois at Chicago, Chicago, Illinois 60607, USA
[52]Northern Illinois University, DeKalb, Illinois 60115, USA
[53]Northwestern University, Evanston, Illinois 60208, USA
[54]Indiana University, Bloomington, Indiana 47405, USA
[55]University of Notre Dame, Notre Dame, Indiana 46556, USA
[56]Purdue University Calumet, Hammond, Indiana 46323, USA
[57]Iowa State University, Ames, Iowa 50011, USA
[58]University of Kansas, Lawrence, Kansas 66045, USA
[59]Kansas State University, Manhattan, Kansas 66506, USA
[60]Louisiana Tech University, Ruston, Louisiana 71272, USA
[61]University of Maryland, College Park, Maryland 20742, USA
[62]Boston University, Boston, Massachusetts 02215, USA
[63]Northeastern University, Boston, Massachusetts 02115, USA
[64]University of Michigan, Ann Arbor, Michigan 48109, USA
[65]Michigan State University, East Lansing, Michigan 48824, USA
[66]University of Mississippi, University, Mississippi 38677, USA
[67]University of Nebraska, Lincoln, Nebraska 68588, USA
[68]Princeton University, Princeton, New Jersey 08544, USA
[69]State University of New York, Buffalo, New York 14260, USA
[70]Columbia University, New York, New York 10027, USA
[71]University of Rochester, Rochester, New York 14627, USA
[72]State University of New York, Stony Brook, New York 11794, USA
[73]Brookhaven National Laboratory, Upton, New York 11973, USA
[74]Langston University, Langston, Oklahoma 73050, USA
[75]University of Oklahoma, Norman, Oklahoma 73019, USA
[76]Oklahoma State University, Stillwater, Oklahoma 74078, USA
[77]Brown University, Providence, Rhode Island 02912, USA
[78]University of Texas, Arlington, Texas 76019, USA
[79]Southern Methodist University, Dallas, Texas 75275, USA
[80]Rice University, Houston, Texas 77005, USA
[81]University of Virginia, Charlottesville, Virginia 22901, USA and
[82]University of Washington, Seattle, Washington 98195, USA

(Dated: April 20, 2008)

We present a measurement of the forward-backward charge asymmetry (A_{FB}) in $p\bar{p} \rightarrow Z/\gamma^* + X \rightarrow e^+e^- + X$ events at a center-of-mass energy of 1.96 TeV using 1.1 fb^{-1} of data collected with the D0 detector at the Fermilab Tevatron collider. A_{FB} is measured as a function of the invariant mass of the electron-positron pair, and found to be consistent with the standard model prediction. We use the A_{FB} measurement to extract the effective weak mixing angle $\sin^2 \theta_W^{\text{eff}} = 0.2327 \pm 0.0018$ (stat.) ± 0.0006 (syst.).

PACS numbers: 13.85.-t, 13.38.Dg, 12.15.Mm, 12.38.Qk

In the standard model (SM), the neutral-current couplings of the Z bosons to fermions (f) are defined as

$$-i\frac{g}{\cos\theta_W}\cdot\bar{f}\gamma^\mu(g_V^f + g_A^f\gamma_5)f\cdot Z_\mu, \quad (1)$$

where θ_W is the weak mixing angle, and g_V^f and g_A^f are the vector and axial-vector couplings with $g_V^f = I_3^f - 2Q_f\sin^2\theta_W$ and $g_A^f = I_3^f$. Here I_3^f is the weak isospin component of the fermion and Q_f its charge. The presence of both vector and axial-vector couplings in $q\bar{q}\to Z/\gamma^*\to\ell^+\ell^-$ gives rise to an asymmetry in the polar angle (θ) of the negatively charged lepton momentum relative to the incoming quark momentum in the rest frame of the lepton pair. The angular differential cross section can be written as

$$\frac{d\sigma}{d\cos\theta} = A(1+\cos^2\theta) + B\cos\theta, \quad (2)$$

where A and B are functions dependent on I_3^f, Q_f, and $\sin^2\theta_W$. Events with $\cos\theta > 0$ are called forward events, and those with $\cos\theta < 0$ are called backward events.

The forward-backward charge asymmetry, A_{FB}, is defined as

$$A_{FB} = \frac{\sigma_F - \sigma_B}{\sigma_F + \sigma_B}, \quad (3)$$

where $\sigma_{F/B}$ is the integral cross section in the forward/backward configuration. We measure A_{FB} as a function of the invariant mass of the lepton pair. To minimize the effect of the unknown transverse momenta of the incoming quarks in the measurement of the forward and backward cross sections, we use θ calculated in the Collins-Soper reference frame [1]. In this frame, the polar axis is defined as the bisector of the proton beam momentum and the negative of the anti-proton beam momentum when they are boosted into the rest frame of the lepton pair.

The forward-backward asymmetry is sensitive to $\sin^2\theta_W^{\text{eff}}$, which is an effective parameter that includes higher order corrections. The current world average value of $\sin^2\theta_W^{\text{eff}}$ is 0.23152 ± 0.00014 [2]. Two $\sin^2\theta_W^{\text{eff}}$ measurements are more than two standard deviations from the world average value: the charge asymmetry for b quark production ($A_{FB}^{0,b}$) from the LEP and SLD collaborations [3] and the measurement of $\sin^2\theta_W^{\text{eff}}$ from the NuTeV collaboration [4]. The $A_{FB}^{0,b}$ measurement is sensitive to the couplings of b quarks to the Z boson, and the NuTeV measurement is sensitive to the couplings of u and d quarks to the Z boson, as is the measurement presented here. In addition, A_{FB} measurements at the Tevatron can be performed up to values of the dilepton mass exceeding those achieved at LEP and SLC, therefore becoming sensitive to possible new physics effects, such as new heavy neutral gauge bosons [5] or extra dimensions [6]. Although direct searches for these new phenomena in the $Z/\gamma^*\to\ell^+\ell^-$ final state have been recently performed by the CDF and D0 Collaborations [7], being sensitive to different combination of couplings, charge asymmetry measurements provide complementary information [8]. Therefore, the combination of both types of analyses will allow to set more model-independent constraints on physics beyond the SM.

The CDF collaboration measured A_{FB} using 108 pb^{-1} of data in Run I [9] and 72 pb^{-1} of data in Run II [10]. This analysis uses 1066 ± 65 pb^{-1} of data [11] collected with the D0 detector [12] at the Fermilab Tevatron collider at a center-of-mass energy of 1.96 TeV to measure the A_{FB} distribution and extract $\sin^2\theta_W^{\text{eff}}$. The D0 detector includes a central tracking system, composed of a silicon microstrip tracker (SMT) and a central fiber tracker (CFT), both located within a 2 T superconducting solenoidal magnet and optimized for tracking and vertexing capabilities at pseudorapidities of $|\eta| < 3$ and $|\eta| < 2.5$ respectively [13]. Three uranium and liquid argon calorimeters provide coverage out to $|\eta|\approx 4.2$: a central calorimeter with coverage of $|\eta| < 1.1$ and two end calorimeters with coverage of $1.5 < |\eta| < 4.2$. A muon system surrounds the calorimetry and consists of three layers of scintillators and drift tubes and 1.8 T iron toroids with coverage of $|\eta| < 2$.

To select Z/γ^* events, we require two isolated electromagnetic (EM) clusters that have shower shapes consistent with that of an electron. EM candidates are required to have transverse momentum $p_T > 25$ GeV. The dielectron pair must have a reconstructed invariant mass $50 < M_{ee} < 500$ GeV. If an event has both its EM candidates in the central calorimeter (CC events), each must be spatially matched to a reconstructed track in the tracking system. Because the tracking efficiency decreases with magnitude of the rapidity in the end calorimeter, events with one candidate in the central and one candidate in the end calorimeter (CE events) are required to have a matching track only for that in the central calorimeter. For CC events, the two candidates are further required to have opposite charges. For CE events, the determination of forward or backward is made according to the charge of the EM candidate in the central calorimeter. A total of 35,626 events remain after application of all selection criteria, with 16,736 CC events and 18,890 CE events. The selection efficiencies are measured using data, and no differences between forward and backward events are observed.

The asymmetry is measured in 14 M_{ee} bins and presented in Table I, which also summarizes number of selected events in each bin. The bin widths are determined by the mass resolution, of order (3−4)%, and event statistics.

M_{ee} range (GeV)	CC Forward	CC Backward	CE Forward	CE Backward
$50-60$	69	78	15	16
$60-70$	104	158	51	91
$70-75$	96	117	64	93
$75-81$	191	235	172	293
$81-86.5$	749	763	843	970
$86.5-89.5$	1388	1357	1860	1694
$89.5-92$	2013	1918	2543	2214
$92-97$	2914	2764	3132	2582
$97-105$	686	549	867	470
$105-115$	153	97	243	88
$115-130$	101	39	167	61
$130-180$	91	33	202	69
$180-250$	31	13	53	16
$250-500$	14	15	17	4

TABLE I: Number of forward and backward events after selection in the CC and CE regions.

Monte Carlo (MC) samples for the $Z/\gamma^* \rightarrow e^+e^-$ process are generated using the PYTHIA event generator [14] using the CTEQ6L1 parton distribution functions (PDFs) [15], followed by a detailed GEANT-based simulation of the D0 detector [16]. To improve the agreement between data and simulation, selection efficiencies determined by the MC are corrected to corresponding values measured in the data. Furthermore, the simulation is tuned to reproduce the calorimeter energy scale and resolution, as well as the distributions of the instantaneous luminosity and z position of the event primary vertex, observed in data. Next-to-leading order (NLO) quantum chromodynamics (QCD) corrections for Z/γ^* boson production [17, 18] are applied by reweighting the Z/γ^* boson transverse momentum, rapidity, and invariant mass distributions from PYTHIA.

The largest background arises from photon+jets and multijet final states in which photons or jets are misreconstructed as electrons. Smaller background contributions arise from electroweak processes that produce two real electrons in the final state. The multijet background is estimated using collider data by fitting the electron isolation distribution in data to the sum of the isolation distributions from a pure electron sample and an EM-like jet sample. The pure electron sample is obtained by enforcing tighter selection criteria on the two electrons with $80 < M_{ee} < 100$ GeV. The EM-like jets sample is obtained from a sample where only one good EM cluster and one jet are back-to-back in azimuthal angle ϕ. The contamination in the EM-like jets sample from $W \rightarrow e\nu$ events is removed by requiring missing transverse energy $\not\!\!E_T < 10$ GeV. The overall multijet background fraction is found to be approximately 0.9% for the whole mass region. Other SM backgrounds due to $Z/\gamma^* \rightarrow \tau^+\tau^-$, $W+\gamma$, W+jets, WW, WZ and $t\bar{t}$ are estimated separately for forward and backward events using PYTHIA events passed through the GEANT simulation. Higher order corrections to the PYTHIA leading order (LO) cross sections have been applied [18–20]. These SM backgrounds are found to be negligible for almost all mass bins.

In the SM, the A_{FB} distribution is fully determined by the value of $\sin^2\theta_W^{\text{eff}}$ in a LO prediction for the process $q\bar{q} \rightarrow Z/\gamma^* \rightarrow \ell^+\ell^-$. The value of $\sin^2\theta_W^{\text{eff}}$ is extracted from the data by comparing the background-subtracted raw A_{FB} distribution with templates corresponding to different input values of $\sin^2\theta_W^{\text{eff}}$ generated with PYTHIA and GEANT-based MC simulation. Using both CC and CE events, we measure $\sin^2\theta_W^{\text{eff}} = 0.2322 \pm 0.0018$ (stat.) $\pm\ 0.0006$ (syst.). The primary systematic uncertainties are due to the PDFs (0.0005) and the EM energy scale and resolution (0.0003). We include higher order QCD and electroweak corrections using the ZGRAD2 [21] program with the generator-level Z/γ^* boson p_T distribution tuned to match our measured distribution [22]. The effect of higher order corrections results in a central value of $\sin^2\theta_W^{\text{eff}} = 0.2327$.

Due to the detector resolution, events may be reconstructed in a different mass bin than the one in which they were generated. The CC and CE raw A_{FB} distributions are unfolded separately and then combined. The unfolding procedure is based on an iterative application of the method of matrix inversion [23]. A response matrix is computed as R_{ij}^{FF} for an event that is measured as forward in M_{ee} bin i to be found as forward and in bin j at the generator level. Likewise, we also calculate the response matrices for backward events being found as backward (R_{ij}^{BB}), forward as backward (R_{ij}^{FB}), and backward as forward (R_{ij}^{BF}). Four matrices are calculated from the GEANT MC simulation and used to unfold the raw A_{FB} distribution. The method was verified by comparing the true and unfolded spectrum generated using pseudo-experiments.

The data are further corrected for acceptance and selection efficiency using the GEANT simulation. The overall acceptance times efficiency rises from 3.5% for $50 < M_{ee} < 60$ GeV to 21% for $250 < M_{ee} < 500$ GeV.

The electron charge measurement in the central calorimeter determines whether an event is forward or backward. Any mismeasurement of the charge of the electron results in a dilution of A_{FB}. The charge misidentification rate, f_Q, is measured using $Z/\gamma^* \rightarrow e^+e^-$ events and the misidentification rate rises from 0.21% at $50 < M_{ee} < 60$ GeV to 0.92% at $250 < M_{ee} < 500$ GeV. The charge misidentification rate is included as a dilution factor $\mathcal{D}$ in A_{FB}, with $\mathcal{D} = (1-2f_Q)/(1-2f_Q+f_Q^2)$ for CC events and $\mathcal{D} = (1-2f_Q)$ for CE events.

The final unfolded A_{FB} distribution using both CC and CE events is shown in Fig. 1, compared to the PYTHIA prediction using the CTEQ6L1 PDFs [15] and the ZGRAD2 prediction using the CTEQ5L PDFs [24]. Both predictions use $\sin^2\theta_W^{\text{eff}} = 0.2322$. The χ^2/d.o.f.

with respect to the PYTHIA prediction is 16.1/14 for CC, 8.5/14 for CE, and 10.6/14 for CC and CE combined. The systematic uncertainties for the unfolded A_{FB} distribution arise from the electron energy scale and resolution, backgrounds, limited MC samples used to calculate the response matrices, acceptance and efficiency corrections, charge misidentification and PDFs. The unfolded A_{FB} together with the PYTHIA and ZGRAD2 predictions for each mass bin can be found in Table II. The correlations between invariant mass bins are shown in Table III.

In conclusion, we have measured the forward-backward charge asymmetry for the $p\bar{p} \to Z/\gamma^* + X \to e^+e^- + X$ process in the dielectron invariant mass range 50 − 500 GeV using 1.1 fb^{-1} data collected by the D0 experiment. The measured A_{FB} values are in good agreement with the SM predictions. We use the A_{FB} distribution to determine $\sin^2\theta_W^{\rm eff} = 0.2327 \pm 0.0018\,({\rm stat.}) \pm 0.0006\,({\rm syst.})$. The precision of this measurement is comparable to that obtained from the combination of LEP measurements of the inclusive hadronic charge asymmetry [3] and that of NuTeV measurement [4]. Our measurement of $\sin^2\theta_W^{\rm eff}$, which is sensitive to Z couplings to electrons and light quarks, agrees well with the world average. With about 8 fb^{-1} of data expected by the end of Run II, a combined measurement of A_{FB} by the CDF and D0 collaborations using electron and muon final states could lead to a measurement of $\sin^2\theta_W^{\rm eff}$ with a precision comparable to that of the current world average. Such measurement would benefit from further improvements to current MC generators incorporating higher order QCD and electroweak corrections.

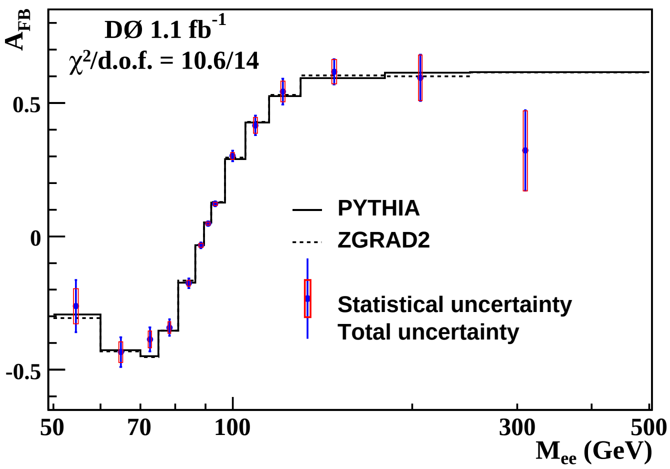

FIG. 1: Comparison between the unfolded A_{FB} (points) and the PYTHIA (solid curve) and ZGRAD2 (dashed line) predictions. The inner (outer) vertical lines show the statistical (total) uncertainty.

$\langle M_{ee}\rangle$ (GeV)	Predicted A_{FB} PYTHIA	ZGRAD2	Unfolded A_{FB}
54.5	−0.293	−0.307	$-0.262 \pm 0.066 \pm 0.072$
64.9	−0.426	−0.431	$-0.434 \pm 0.039 \pm 0.040$
72.6	−0.449	−0.452	$-0.386 \pm 0.032 \pm 0.031$
78.3	−0.354	−0.354	$-0.342 \pm 0.022 \pm 0.022$
84.4	−0.174	−0.166	$-0.176 \pm 0.012 \pm 0.014$
88.4	−0.033	−0.031	$-0.034 \pm 0.007 \pm 0.008$
90.9	0.051	0.052	$0.048 \pm 0.006 \pm 0.005$
93.4	0.127	0.129	$0.122 \pm 0.006 \pm 0.007$
99.9	0.289	0.296	$0.301 \pm 0.013 \pm 0.015$
109.1	0.427	0.429	$0.416 \pm 0.030 \pm 0.022$
121.3	0.526	0.530	$0.543 \pm 0.039 \pm 0.028$
147.9	0.593	0.603	$0.617 \pm 0.046 \pm 0.013$
206.4	0.613	0.600	$0.594 \pm 0.085 \pm 0.016$
310.5	0.616	0.615	$0.320 \pm 0.150 \pm 0.018$

TABLE II: The first column shows the cross section weighted average of the invariant mass in each mass bin derived from PYTHIA. The second and third columns show the A_{FB} predictions from PYTHIA and ZGRAD2. The last column is the unfolded A_{FB}; the first uncertainty is statistical, and the second is systematic.

We thank the staffs at Fermilab and collaborating institutions, and acknowledge support from the DOE and NSF (USA); CEA and CNRS/IN2P3 (France); FASI, Rosatom and RFBR (Russia); CNPq, FAPERJ, FAPESP and FUNDUNESP (Brazil); DAE and DST (India); Colciencias (Colombia); CONACyT (Mexico); KRF and KOSEF (Korea); CONICET and UBACyT (Argentina); FOM (The Netherlands); STFC (United Kingdom); MSMT and GACR (Czech Republic); CRC Program, CFI, NSERC and WestGrid Project (Canada); BMBF and DFG (Germany); SFI (Ireland); The Swedish Research Council (Sweden); CAS and CNSF (China); and the Alexander von Humboldt Foundation.

[a] Visitor from Augustana College, Sioux Falls, SD, USA.
[b] Visitor from The University of Liverpool, Liverpool, UK.
[c] Visitor from ICN-UNAM, Mexico City, Mexico.
[d] Visitor from II. Physikalisches Institut, Georg-August-University, Göttingen, Germany.
[e] Visitor from Helsinki Institute of Physics, Helsinki, Finland.
[f] Visitor from Universität Zürich, Zürich, Switzerland.
[‡] Deceased.

[1] J.C. Collins and D.E. Soper, Phys. Rev. D **16**, 2219 (1977).
[2] W.-M. Yao *et al.* (Particle Data Group), J. Phys. G **33**, 1 (2006).
[3] G. Abbiendi *et al.* (LEP Collaborations ALEPH, DELPHI, L3 and OPAL; SLD Collaboration, LEP Electroweak Working Group, SLD Electroweak and Heavy Flavor Groups), Phys. Rep. **427**, 257 (2006).

Mass bin	1	2	3	4	5	6	7	8	9	10	11	12	13	14
1	1.00	0.21	0.04	0.00	0.00	0.01	0.00	0.01	0.00	0.00	0.00	0.00	0.00	0.00
2		1.00	0.42	0.08	0.02	0.01	0.02	0.01	0.00	0.00	0.00	0.00	0.00	0.00
3			1.00	0.49	0.13	0.04	0.03	0.02	0.01	0.00	0.00	0.00	0.00	0.00
4				1.00	0.52	0.16	0.08	0.04	0.01	0.00	0.00	0.00	0.00	0.00
5					1.00	0.72	0.32	0.11	0.01	0.00	0.00	0.00	0.00	0.00
6						1.00	0.79	0.40	0.03	0.00	0.00	0.00	0.00	0.00
7							1.00	0.80	0.15	0.01	0.00	0.00	0.00	0.00
8								1.00	0.50	0.04	0.00	0.00	0.01	0.00
9									1.00	0.38	0.04	0.00	0.00	0.00
10										1.00	0.30	0.01	0.00	0.00
11											1.00	0.14	0.00	0.00
12												1.00	0.06	0.00
13													1.00	0.06
14														1.00

TABLE III: Correlation coefficients between different M_{ee} mass bins. Only half of the symmetric correlation matrix is presented.

[4] G.P. Zeller *et al.* (NuTeV Collaboration), Phys. Rev. Lett. **88**, 091802 (2002); **90**, 239902(E) (2003).

[5] J.L. Rosner, Phys. Rev. D **54**, 1078 (1996); M. Carena *et al.*, Phys.Rev. D **70** 093009 (2004).

[6] H. Davoudiasl, J.L. Hewett, and T.G. Rizzo, Phys. Rev. Lett. **84**, 2080 (2000).

[7] A. Abulencia *et al.* (CDF Collaboration), Phys. Rev. Lett. **95**, 252001 (2005); D. Acosta *et al.* (CDF Collaboration), Phys. Rev. Lett. **95**, 131801 (2005); V. Abazov *et al.* (D0 Collaboration), Phys. Rev. Lett. **95**, 091801 (2005); V. Abazov *et al.* (D0 Collaboration), Phys. Rev. Lett. **95**, 161602 (2005); T. Aaltonen *et al.* (CDF Collaboration), Phys. Rev. Lett. **99**, 171802 (2007); V. Abazov *et al.* (D0 Collaboration), Phys. Rev Lett. **100**, 091802 (2008).

[8] A. Abulencia *et al.* (CDF Collaboration), Phys. Rev. Lett. **96**, 211801 (2006).

[9] T. Affolder *et al.* (CDF Collaboration), Phys. Rev. Lett. **87**, 131802 (2001); F. Abe *et al.* (CDF Collaboration), Phys. Rev. Lett. **77**, 2616 (1996).

[10] D. Acosta *et al.* (CDF Collaboration), Phys. Rev. D **71**, 052002 (2005).

[11] T. Andeen *et al.*, FERMILAB-TM-2365 (2007).

[12] V. Abazov *et al.* (D0 Collaboration), Nucl. Instrum. Methods Phys. Res., Sect. A **565**, 463 (2006).

[13] $\eta = -\ln[\tan(\theta/2)]$, where θ is the polar angle measured relative to the proton beam direction.

[14] T. Sjöstrand *et al.*, Comput. Phys. Commun. **135**, 238 (2001). PYTHIA version v6.323 is used throughout.

[15] J. Pumplin *et al.*, JHEP **0207**, 012 (2002); D. Stump *et al.*, JHEP **0310**, 046 (2003).

[16] R. Brun and F. Carminati, CERN Program Library Long Writeup W5013, 1993 (unpublished).

[17] C. Balazs and C.P. Yuan, Phys. Rev. D **56**, 5558 (1997).

[18] R. Hamberg, W.L. van Neerven, and T. Matsuura, Nucl. Phys. **B359**, 343 (1991); **644**, 403(E) (2002).

[19] J.M. Campbell and R.K. Ellis, Phys. Rev. D **60**, 113006 (1999).

[20] N. Kidonakis and R. Vogt, Phys. Rev. D **68**, 114014 (2003); M. Cacciari *et al.*, JHEP **04**, 68 (2004).

[21] U. Baur, S. Keller, and W.K. Sakumoto, Phys. Rev. D **57**, 199 (1998); U. Baur *et al.*, Phys. Rev. D **65**, 033007 (2002).

[22] V. Abazov *et al.* (D0 Collaboration), Phys. Rev. Lett. **100**, 102002 (2008).

[23] G.L. Marchuk, Methods of Numerical Mathematics (Springer, Berlin, 1975).

[24] H.L. Lai *et al.*, Eur. Phys. J. C **12**, 375 (2000).